6-1991

Onset of Convection for Autocatalytic Reaction Fronts: Laterally Bounded Systems

D. A. Vasquez

Boyd F. Edwards
Utah State University

J. W. Wilder

Recommended Citation
"Onset of Convection for Autocatalytic Reaction Fronts: Laterally Bounded Systems," D. A. Vasquez, B. F. Edwards, and J. W. Wilder, Phys. Rev. A 43, 6694 (1991) [41].

Onset of convection for autocatalytic reaction fronts: Laterally bounded systems

Desiderio A. Vasquez, Boyd F. Edwards, and Joseph W. Wilder
Department of Physics and Department of Mathematics, West Virginia University, Morgantown, West Virginia 26506
(Received 26 September 1990; revised manuscript received 6 March 1991)

Linear hydrodynamics yields the onset of convection for ascending autocatalytic reaction fronts in laterally bounded geometries. The system is studied in the limit of infinite and zero thermal diffusivity. For convection in a vertical slab of thickness a or a long vertical cylinder of radius a, the appropriate dimensionless driving parameter $\mathcal{S}=\delta g a^3/\nu D_c$ involves the fractional density difference δ between the unreacted and reacted fluids, the acceleration of gravity g, the kinematic viscosity ν, and the catalyst molecular diffusivity D_c. Calculated critical values $\mathcal{S}_c$ for onset of convection agree with recent experiments on iodate–arsenous acid systems. We also show that, compared with the unbounded system, the sidewalls tend to suppress convection.

I. INTRODUCTION

Recent experiments near autocatalytic reaction fronts[1–8] require corresponding calculations for convection in laterally bounded geometries. In these experiments, the speed of propagation of the front is limited by the molecular diffusion of the catalyst into the unreacted fluid. Such self-sustaining or "autocatalytic" reaction fronts produce both thermal and concentration gradients in the vicinity of the reaction front, leading to potentially unstable density gradients.

Previous calculations of the onset of convection in unbounded geometries consider limiting cases of the stability problem. In the limits of zero and infinite thermal diffusivity D_T,[9] a thin reaction front separates two distinct fluids each of uniform density, the stability of the front being governed by the discontinuous jump in density at the front. For parameter values relevant to experiments on iodate–arsenous acid solutions and for an ascending planar horizontal front with the heavier fluid above the front, these calculations predict convection for perturbation wavelengths exceeding a critical wavelength λ_c, with $\lambda_c=0.99$ mm for $D_T=0$ and $\lambda_c=1.29$ mm for for $D_T\to\infty$. These results indicate that thermal gradients may play a small role at onset of convection compared with the density discontinuity. The large value $\lambda_c\approx 7$ mm for a separate calculation[10] neglecting the density discontinuity but including thermal gradients for finite D_T confirms the conclusion that thermal gradients play a small role at onset of convection. We expect that a full calculation including both the density discontinuity and the thermal gradients will yield a critical wavelength near 1 mm.

To facilitate comparison with experiments, we consider the onset of convection for an ascending front separating two incompressible fluids for laterally bounded geometries. The densities of the unreacted and reacted fluids can each be considered to be uniform when the chemical reaction front is thin and the thermal diffusivity D_T is either small or large. For an unreacted fluid at initial temperature T_0 and density ρ_0 and a reacted fluid at final temperature T_1 under adiabatic conditions, large D_T implies a uniform fluid temperature T_1 except far ahead of the reaction front, with the corresponding uniform densities denoted by ρ_1 and $\tilde{\rho}_1$ in the unreacted and reacted fluids. The corresponding fractional density difference $\delta_1=\rho_1/\tilde{\rho}_1-1$ is due solely to compositional differences between the unreacted and reacted fluids. Small D_T relegates all thermal gradients to the thin reaction front, implying a sudden change in temperature from T_0 to T_1 as the fluid passes through the front. In this case, the fractional density difference $\delta_0=\rho_0/\tilde{\rho}_1-1$ includes both thermally induced and compositionally induced density differences, which are typically of the same order in the experiments.[9] It is convenient to define a general fractional density difference $\delta=\rho/\tilde{\rho}-1$ between the incompressible unreacted and reacted fluids of densities ρ and $\tilde{\rho}$, which can be replaced by either δ_0 or δ_1 to compare with experiments. We here consider insulated sidewalls. Below, we write the equations of motion for the onset of convection using the thin front approximation developed in Ref. 9, which treats the front as a surface of discontinuity. To develop techniques and test approximations, we first study the onset of convection between two parallel vertical planes of separation a. We then proceed to study the onset of axisymmetric convection for long vertical cylinders of radius a. Finally, we compare these results with experiments on iodate–arsenous acid mixtures.

II. EQUATIONS OF MOTION

The dimensionless hydrodynamic equations

$$\frac{\partial \mathbf{v}}{\partial t}+(\mathbf{v}\cdot\nabla)\mathbf{v}=-\nabla p+\nabla^2\mathbf{v}\ , \tag{1}$$

$$\nabla\cdot\mathbf{v}=0 \tag{2}$$

express conservation of momentum and mass in incompressible unreacted and reacted fluids, with length and time measured in convenient units of a and a^2/ν, where ν is the kinematic viscosity. The gravity term in Eq. (1) has been absorbed into the reduced pressure

term.[9] There is no equation for the temperature since we treat only the limiting cases with large or small thermal diffusivity. In a coordinate frame stationary with respect to an ascending flat horizontal front, the fluid velocity $\mathbf{v}(\mathbf{x},t)=-v_0\hat{\mathbf{z}}$ in the absence of convection reflects fluid flow through the front as unreacted fluid is converted to reacted fluid, where $v_0=c_0a/\nu$ is a dimensionless flat front speed and $\hat{\mathbf{z}}$ is a unit vector pointing up. In this frame, impenetrable no-slip sidewalls, called rigid boundary conditions, therefore demand that $\mathbf{v}=-v_0\hat{\mathbf{z}}$ at the sidewalls, whereas all components of fluid velocity must be continuous across the reaction front. Momentum balance at the front requires the tangential stress $\epsilon_{ijk}n_jn_lT_{kl}$ to be continuous across the front (Ref. 9), where ϵ_{ijk} is the totally antisymmetric tensor, the n_i are the Cartesian components of the unit normal vector $\hat{\mathbf{n}}$ to the front pointing into the unreacted fluid, sums over repeated indices are implied, and

$$T_{ij}=-\frac{\partial v_i}{\partial x_j}-\frac{\partial v_j}{\partial x_i} \tag{3}$$

is the (dimensionless) viscous stress tensor. Momentum balance normal to the front requires a discontinuous pressure jump[9]

$$[p]_-^+=-\mathcal{S}\mathcal{D}_ch-[n_in_jT_{ij}]_-^+ \tag{4}$$

owing to the impulsive acceleration caused by the sudden density change experienced by fluid elements as they pass through the front, where $[q]_-^+=q_+-q_-$ is the difference in a quantity q evaluated on the reacted (+) and unreacted (−) sides of the front. Equation (4) involves a dimensionless catalyst diffusivity $\mathcal{D}_c=D_c/\nu$ and a driving parameter

$$\mathcal{S}=\delta ga^3/\nu D_c \tag{5}$$

proportional to the acceleration g of gravity and the fractional density difference δ, indicating increasing tendency to convection for increasing $\mathcal{S}$. Here, $z=h(x,y,t)$ gives the height of the reaction front (in the comoving frame) as a function of the horizontal coordinates and the time, so that $\hat{\mathbf{n}}$ can be written as

$$\hat{\mathbf{n}}=\pm\frac{(\hat{\mathbf{z}}-\nabla h)}{(1+|\nabla h|^2)^{1/2}}\ , \tag{6}$$

where the + sign is relevant when the unreacted fluid is above the front (for upward propagation).

The normal component of the local front propagation speed,[9]

$$\hat{\mathbf{n}}\cdot\hat{\mathbf{z}}\frac{\partial h}{\partial t}=v_0+\mathcal{D}_c\kappa+\hat{\mathbf{n}}\cdot\mathbf{v}_-\ , \tag{7}$$

contains contributions from the local curvature κ and from the fluid velocity $\mathbf{v}_-$ on the unreacted side of the front. Since κ is measured as positive when the center of curvature is in the unreacted fluid, the curvature contribution (proportional to $\mathcal{D}_c$) tends to flatten the reaction front with time, thus tending to stabilize a planar front. The competing effect of buoyancy tends to amplify any deviations from a flat front when the heavier fluid is above the front. Thus, $\mathcal{S}$ measures the strength of buoyancy relative to the stabilizing effect of curvature, and plays a role analogous to the Rayleigh number for buoyancy-driven convection in a fluid heated from below.[11,12]

To study the onset of convection, we introduce small time-dependent perturbations about an ascending convectionless horizontal planar front located at $z=0$ (in the comoving frame) which is described by $\mathbf{v}^{(0)}=-v_0\hat{\mathbf{z}}$, $h^{(0)}=0$, and $\hat{\mathbf{n}}^{(0)}=\hat{\mathbf{z}}$. Accordingly, we write

$$\begin{aligned} h&=h^{(1)}\ ,\\ \mathbf{v}&=\mathbf{v}^{(0)}+\mathbf{v}^{(1)}\ ,\\ p&=p^{(0)}+p^{(1)}\ , \end{aligned} \tag{8}$$

along with similar expressions for $\hat{\mathbf{n}}$, κ, and T_{ij}. Substituting these expressions into Eqs. (1), (2), and (7) and linearizing in the perturbations yields

$$\partial_t\mathbf{v}^{(1)}-v_0\partial_z\mathbf{v}^{(1)}=-\nabla p^{(1)}+\nabla^2\mathbf{v}^{(1)}\ , \tag{9a}$$

$$\nabla\cdot\mathbf{v}^{(1)}=0\ , \tag{9b}$$

$$\partial_th^{(1)}=\mathcal{D}_c\kappa^{(1)}+w_-^{(1)}\ , \tag{9c}$$

with $w=\hat{\mathbf{z}}\cdot\mathbf{v}$ denoting the vertical component of velocity. Correspondingly, rigid boundary conditions require $\mathbf{v}^{(1)}$ to vanish at the sidewalls and

$$[\mathbf{v}^{(1)}]_-^+=0\ , \tag{9d}$$

$$[\epsilon_{i3k}T_{k3}^{(1)}]_-^+=0\ , \tag{9e}$$

$$[p^{(1)}]_-^+=-\mathcal{S}\mathcal{D}_ch^{(1)}+2[\partial_zw^{(1)}]_-^+\ , \tag{9f}$$

where $\hat{\mathbf{z}}\cdot\hat{\mathbf{n}}^{(1)}=0$ because $\nabla h^{(1)}$ is horizontal. Equations (9) govern the time evolution of small perturbations about a flat front.

Marginal stability of the flat front occurs when the perturbations neither grow nor decay with time,[9] that is, when buoyancy and curvature effects balance each other. Accordingly, we can obtain a critical driving parameter $\mathcal{S}_c$ for the onset of convection by setting $\partial_t=0$ and $\mathcal{S}=\mathcal{S}_c$ in Eqs. (9).

III. VERTICAL SLAB

Before proceeding to the more complicated cylindrical geometry, we study the two-dimensional marginal stability of a vertical slab of width a defined by $-\frac{1}{2}\le x\le\frac{1}{2}$ in dimensionless units. This will help us to develop the mathematical framework and justify approximations for the cylindrical problem. For two-dimensional motion in the x-z plane the continuity equation (9b) allows us to introduce a vector potential $\mathbf{A}=A(x,z)\hat{\mathbf{y}}$ such that $\mathbf{v}^{(1)}=\nabla\times\mathbf{A}$. Taking the curl of Eq. (9a) we obtain an equation for A at marginal stability,

$$v_0\frac{\partial}{\partial z}\nabla^2A+\nabla^2(\nabla^2A)=0\ . \tag{10a}$$

Replacing the velocity components with their relations to the potential A, Eqs. (9d) and (9e) and the horizontal component of Eq. (9f) yield the corresponding jump conditions on A,

$$[A]_-^+=0\ , \tag{10b}$$

$$[\partial_z A]_-^+=0\ , \tag{10c}$$

$$[\partial_z^2 A]_-^+=0\ , \tag{10d}$$

$$[\partial_z^3 A]=\mathcal{S}_c\mathcal{D}_c\partial_x h^{(1)}\ , \tag{10e}$$

where the horizontal component of the momentum equation (9a) has been used to simplify Eq. (10e). Since these conditions are already of first order in the deviations about the ascending flat front at $z=0$, we take

$$[q]_-^+=\lim_{\epsilon\to 0}(q|_{z=-\epsilon}-q|_{z=\epsilon})\ .$$

The curvature κ is given by $\kappa^{(1)}=\partial_x^2 h^{(1)}$ to first order in h and (9c) gives

$$\mathcal{D}_c\partial_x^2 h^{(1)}+\partial_x A|_-=0\ . \tag{10f}$$

Rigid boundary conditions require A and its normal derivative to vanish at the walls. To satisfy these boundary conditions we write A as

$$A(x,z)=\sum_{m=1}^{\infty}\mathcal{F}_m(z)\mathcal{T}_m(x)\ . \tag{11}$$

The functions $\mathcal{F}_m$ will be determined below and the functions $\mathcal{T}_m$ are a complete set of orthonormal solutions of

$$\frac{d^4}{dx^4}\mathcal{T}_m=\lambda_m^4\mathcal{T}_m \tag{12}$$

satisfying $\mathcal{T}_m=d\mathcal{T}_m/dx=0$ at $x=\pm\frac{1}{2}$. The eigenfunctions $\mathcal{T}_m$ are divided into two classes: C_m for even functions and S_m for odd functions. The functions and their eigenvalues λ_m are tabulated by Chandrasekar.[13] We substitute this expansion into (10a) and obtain

$$\sum_{m=1}^{N}\left[\left(\frac{d^4}{dz^4}+\lambda_m^4+v_0\frac{d^3}{dz^3}\right)\delta_{mn}+2(\mathcal{T}_m''|\mathcal{T}_n)\frac{d^2}{dz^2}+v_0(\mathcal{T}_m''|\mathcal{T}_n)\frac{d}{dz}\right]\mathcal{F}_m(z)=0\ , \tag{13}$$

where

$$(\mathcal{T}_m''|\mathcal{T}_n)=\int_{-1/2}^{1/2}\frac{d^2\mathcal{T}_m}{dx^2}\mathcal{T}_n dx$$

has been tabulated by Reid and Harris.[14] Here, we have truncated the infinite expansion on A to N terms to yield a set of N coupled ordinary differential equations. Our procedure entails finding the eigenvalues and eigenvectors for the equations on $\mathcal{F}_m$ [Eq. (13)], substituting a linear combination of them into Eq. (11), and then determining the coefficients using the jump conditions [Eqs. (10)]. We look for eigenvectors of the form

$$\mathcal{F}_m=F_m e^{kz}\ \text{ for } m=1,2,\ldots,N\ , \tag{14}$$

where the F_m are constants. This leads to the following system of equations:

$$\begin{bmatrix} m_{11} & m_{12} & \cdots & m_{1N}\\ m_{21} & m_{22} & \cdots & m_{2N}\\ \vdots & \vdots & \ddots & \vdots\\ m_{N1} & n_{N2} & \cdots & m_{NN}\end{bmatrix}\begin{bmatrix}F_1\\F_2\\\vdots\\F_N\end{bmatrix}=0\ , \tag{15}$$

where

$$m_{ij}=\begin{cases}k^4+v_0k^3+2(\mathcal{T}_i''|\mathcal{T}_i)k^2+v_0(\mathcal{T}_i''|\mathcal{T}_i)k+\lambda_i^4 & \text{if } i=j\\ 2(\mathcal{T}_j''|\mathcal{T}_i)k^2+v_0(\mathcal{T}_j''|\mathcal{T}_i)k & \text{if } i\neq j\ .\end{cases} \tag{16}$$

Our goal is to obtain the critical distance a_c from the jump conditions, Eqs. (10). Since the eigenvalues k depend on $v_0=c_0a_c/\nu$, we follow a self-consistent procedure: we take a reasonable value of v_0, evaluate the k's, and obtain a_c. This a_c defines a new value $v_0=c_0a_c/\nu$ to be used in the next iteration. We repeat the process until v_0 remains constant. All the other parameters are given in Sec. V. We proceed now to obtain the eigenvalues. The system (15) has a nontrivial solution when the determinant of the matrix is zero. This leads to a polynomial equation of order $4N$ on k. Half of the roots k_i of this polynomial (labeled $i=1,2,\ldots,2N$) have negative real parts and half (labeled $i=2N+1,2N+2,\ldots,4N$) have positive real parts. The eigenvector corresponding to the eigenvalue k_i is denoted by $(F_{1i},F_{2i},\ldots,F_{Ni})$. Since we require that the solution vanish as $z\to\pm\infty$ the general solution for $A(x,z)$ has the form

$$A(x,z)=\begin{cases}\displaystyle\sum_{i=1}^{2N}\sum_{j=1}^{N}\alpha_i F_{ji}\mathcal{T}_j(x)e^{k_i z} & \text{if } z\geq 0\\ \displaystyle\sum_{i=2N+1}^{4N}\sum_{j=1}^{N}\alpha_i F_{ji}\mathcal{T}_j(x)e^{k_i z} & \text{if } z<0\ .\end{cases} \tag{17}$$

The jump conditions lead to a homogeneous linear system with unknown coefficients α_m;

$$\sum_{i=1}^{2N}\alpha_i F_{ji}-\sum_{i=2N+1}^{4N}\alpha_i F_{ji}=0\ , \tag{18a}$$

$$\sum_{i=1}^{2N}\alpha_i k_i F_{ji}-\sum_{i=2N+1}^{4N}\alpha_i k_i F_{ji}=0\ , \tag{18b}$$

$$\sum_{i=1}^{2N}\alpha_i k_i^2 F_{ji}-\sum_{i=2N+1}^{4N}\alpha_i k_i^2 F_{ji}=0\ , \tag{18c}$$

$$\sum_{i=1}^{2N}\alpha_i k_i^3 F_{ji}-\sum_{i=2N+1}^{4N}\alpha_i (k_i^3-\mathcal{S}_c)F_{ji}=0 \quad \text{for } j=1,2,\ldots,N\ . \tag{18d}$$

The first three equations come from (10b), (10c), and (10d), while the last one is obtained from both (10e) and (10f). Setting the determinant to zero yields the value of $\mathcal{S}_c$ numerically.

As we mentioned before, the basis functions $\mathcal{T}_m$ have even and odd parity. The matrix element $(\mathcal{T}_m''|\mathcal{T}_n)$ is zero for functions of opposite parity; therefore, we need only to consider bases made up of either $C_m(x)$ or $S_m(x)$. For odd basis functions $\mathcal{T}_m=S_m$ the critical value $\mathcal{S}_c$ is

1810.4851 for a one-term truncation, 1806.5636 for two terms, and 1805.5420 for three. Since the change in $\mathcal{S}_c$ is small we stop here and do not consider four or more functions. For even basis functions $\mathcal{T}_m = C_m$, we obtain $\mathcal{S}_c = 372.6408$, 371.6805, and 371.5382 for the one-, two-, and three-term truncations. The value for $\mathcal{S}_c$ is lower for even functions so they will determine the onset of convection. If we set v_0 equal to zero, $\mathcal{S}_c$ becomes 371.5366 for the three-function basis, which is a change much smaller than the inclusion of the third term in the basis. Therefore, we can neglect the first term in Eq. (10a) without altering the results significantly. This is consistent with the fact that in the laterally unbounded system the solutions do not depend significantly on c_0 (Ref. 9). The relation $\mathcal{S}_c = \delta g a_c^3/\nu D_c$ yields a critical wall separation $a_c = 0.929$ mm for large thermal diffusivity ($\delta = \delta_1$) and $a_c = 0.716$ mm for small thermal diffusivity ($\delta = \delta_0$). The value for a_c should be compared with half the critical wavelength of the unbounded system which lies between 0.49 and 0.64 mm (Ref. 9). The critical length a_c is larger in the bounded system because the walls give additional stability.

IV. CYLINDER

In the previous section we found that the constant v_0 can be set to zero for our purposes. We restrict our study to axisymmetric flows observed in the experiments.[1] The vector potential $\mathbf{A}$ in cylindrical coordinates can be written as $\mathbf{A} = \chi(r,z)\hat{\theta}$ for axisymmetric flows with components of $\mathbf{v}^{(1)}$ given by

$$v_r^{(1)} = -\partial_z \chi \ , \qquad v_z^{(1)} = \frac{1}{r}\partial_r (r\chi) \ . \tag{19}$$

The equation for χ analogous to (10a) is

$$\mathbf{A} = \chi(r,z)\hat{\theta} \ , \qquad (\mathcal{D}_r + \partial_z^2)^2 \chi = 0 \ , \tag{20a}$$

where

$$\mathcal{D}_r = \partial_r \frac{1}{r}\partial_r r \ .$$

The jump conditions (10b)–(10e) become

$$[\chi]_-^+ = 0 \ , \tag{20b}$$

$$[\partial_z \chi]_-^+ = 0 \ , \tag{20c}$$

$$[\partial_z^2 \chi]_-^+ = 0 \ , \tag{20d}$$

$$[\partial_z^3 \chi]_-^+ = \mathcal{S}_c \mathcal{D}_c \partial_r h^{(1)} \ . \tag{20e}$$

Using the curvature of a surface of revolution,[15] it is found that

$$\kappa^{(1)} = \partial_r^2 h^{(1)} + \frac{1}{r}\partial_r h^{(1)}$$

to first order in $h^{(1)}$ and Eq. (9c) becomes

$$\partial_r^2 h^{(1)} + \frac{1}{r}\partial_r h^{(1)} = -\frac{1}{r}\partial_r r\chi \Big|_- \ . \tag{20f}$$

Vanishing velocity components at the walls and vanishing velocity components at the origin imply the following boundary conditions:

$$\chi = \begin{cases} \dfrac{1}{r}\partial_r r\chi = 0 & \text{at } r = 1 \\ 0 & \text{at } r = 0 \ . \end{cases} \tag{21}$$

To solve Eq. (20a) subject to these boundary conditions, we consider a set of orthonormal expansion functions $\mathcal{R}_m$ satisfying

$$\mathcal{D}_r^2 \mathcal{R}_m(r) = \alpha_m^4 \mathcal{R}_m(r) \tag{22}$$

and

$$\mathcal{R}_m(0) = \mathcal{R}_m(1) = \frac{1}{r}\frac{d}{dr} r\mathcal{R}_m(r) \Big|_1 = 0 \ . \tag{23}$$

The functions $\mathcal{R}_m$ are analogous to the functions $\mathcal{T}_m$ that were used for the vertical slab. We can satisfy these conditions by a linear combination of a Bessel function J_1 and a modified Bessel function I_1,

$$\mathcal{R}_m(r) = \frac{J_1(\alpha_m r)}{J_1(\alpha_m)} - \frac{I_1(\alpha_m r)}{I_1(\alpha_m)} \ , \tag{24}$$

which obeys the orthonormality condition

$$\int_0^1 r\mathcal{R}_m \mathcal{R}_n dr = \delta_{mn} \ . \tag{25}$$

The first three eigenvalues are $\alpha_1 = 4.610\,900$, $\alpha_2 = 7.799\,274$, and $\alpha_3 = 10.958\,07$. The expansion for χ analogous to Eq. (11) is

$$\chi(r,z) = \sum_m \mathcal{G}_m(z)\mathcal{R}_m(r) \ . \tag{26}$$

We substitute this expansion into Eq. (20a) to obtain a set of ordinary differential equations for $\mathcal{G}_m$,

$$\sum_m \left[\frac{d^4}{dz^4}\delta_{mn} + \lambda^4 \delta_{mn} + 2(\mathcal{R}_m'' | \mathcal{R}_n)\frac{d^2}{dz^2} \right] \mathcal{G}_m = 0 \ , \tag{27}$$

where

$$(\mathcal{R}_m'' | \mathcal{R}_n) = \int_0^1 r\mathcal{R}_n \mathcal{D}_r \mathcal{R}_m dr \ . \tag{28}$$

This integral can be calculated analytically and the result is

$$(\mathcal{R}_m'' | \mathcal{R}_n) = \begin{cases} \dfrac{4\alpha_m^2 \alpha_n^2}{\alpha_m^4 - \alpha_n^4}\left[\alpha_m \dfrac{I_0(\alpha_m)}{I_1(\alpha_m)} - \alpha_n \dfrac{I_0(\alpha_n)}{I_1(\alpha_n)} \right] & \text{if } m \neq n \\ \alpha_m \dfrac{I_0(\alpha_m)}{I_1(\alpha_m)}\left[2 - \alpha_m \dfrac{I_0(\alpha_m)}{I_1(\alpha_m)} \right] & \text{if } m = n \ . \end{cases} \tag{29}$$

This system of equations is the same as (13) with $v_0=0$, so we proceed to solve it in the same way. Again, the expansion (26) is truncated to include only the first N terms. We look for eigenvectors of the form

$$\mathcal{G}_m = G_m e^{kz} \text{ for } m=1,2,\ldots,N \ . \tag{30}$$

The coefficients G_m are the components of an eigenvector that satisfies

$$\begin{bmatrix} l_{11} & l_{12} & \cdots & l_{1N} \\ l_{21} & l_{22} & \cdots & l_{2N} \\ \vdots & \vdots & \ddots & \vdots \\ l_{N1} & l_{N2} & \cdots & l_{NN} \end{bmatrix} \begin{bmatrix} G_1 \\ G_2 \\ \vdots \\ G_N \end{bmatrix} = 0 \ , \tag{31}$$

where

$$l_{ij} = \begin{cases} k^4 + 2(\mathcal{R}_i''|\mathcal{R}_j)k^2 + \alpha_i^4 & \text{if } i=j \\ 2(\mathcal{R}_i''|\mathcal{R}_j)k^2 & \text{if } i\neq j \ . \end{cases} \tag{32}$$

Once again, we obtain $4N$ values of k that make the determinant equal to zero. We label them k_i as before, such that the real part of k_i is less than zero for $i=1,2,\ldots,2N$ and greater than zero for $i=2N+1,2N+2,\ldots,4N$. Since the velocity must vanish as $z\to\pm\infty$, the general solution for $\chi(r,z)$ has the form

$$\chi(r,z) = \begin{cases} \sum_{i=1}^{2N}\sum_{j=1}^{N} \beta_i G_{ji} \mathcal{R}_j(r) e^{k_i z} & \text{if } z \geq 0 \\ \sum_{i=2N+1}^{4N}\sum_{j=1}^{N} \beta_i G_{ji} \mathcal{R}_j(r) e^{k_i z} & \text{if } z < 0 \ . \end{cases} \tag{33}$$

The jump conditions provide a set of linear equations for the coefficients β,

$$\sum_{i=1}^{2N} \beta_i G_{ji} - \sum_{i=2N+1}^{4N} \beta_i G_{ji} = 0 \ , \tag{34a}$$

$$\sum_{i=1}^{2N} \beta_i k_i G_{ji} - \sum_{i=2N+1}^{4N} \beta_i k_i G_{ji} = 0 \ , \tag{34b}$$

$$\sum_{i=1}^{2N} \beta_i k_i^2 G_{ji} - \sum_{i=2N+1}^{4N} \beta_i k_i^2 G_{ji} = 0 \ , \tag{34c}$$

$$\sum_{i=1}^{2N} \beta_i k_i^3 G_{ji} - \sum_{i=2N+1}^{4N} \beta_i (k_i^3 - \mathcal{S}_c) G_{ji} = 0 \quad \text{for } j=1,2,\ldots,N \ . \tag{34d}$$

Demanding that the determinant of the matrix vanish yields $\mathcal{S}_c=370.9817$, 370.2871, and 370.0810 for the one-, two-, and three-function bases. We find that the convergence is faster than for the vertical slab. Figure 1 shows the resulting velocity field for the one-term truncation.

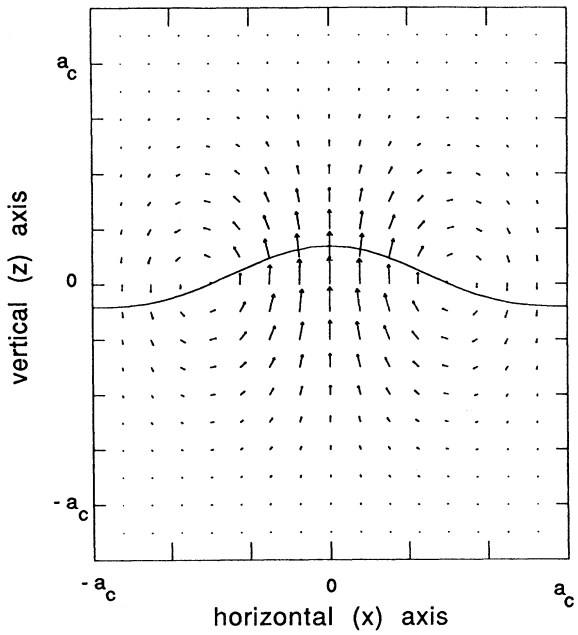

FIG. 1. Velocity field at the onset of convection in a cross section through the axis of a vertical tube. The velocity field is axisymmetric and decays exponentially in the vertical direction. The solid line represents the boundary between chemical species.

V. SUMMARY AND DISCUSSION

For uniform reacted and unreacted fluids, linear hydrodynamics predicts convection near autocatalytic reaction fronts for $\mathcal{S}>\mathcal{S}_c$, with $\mathcal{S}_c=371.5$ for two-dimensional convection in a vertical slab of thickness a and $\mathcal{S}_c=370.1$ for axisymmetric convection in a vertical tube of radius a. These universal critical values are independent of all fluid parameters including the dimensionless catalyst diffusivity $\mathcal{D}_c=D_c/\nu$ and the dimensionless flat front propagation speed $v_0=c_0 a/\nu$. Accordingly, the relation $\mathcal{S}_c=\delta g a_c^3/\nu D_c$ and experimental values of δ, g, ν, and D_c yield the predicted critical radius a_c for onset of convection to be compared with experiments.

Recent experiments on ascending iodate–arsenous acid reaction fronts[1] observe no convection in a tube of diameter $d=0.94$ mm and convection in tubes with $d\geq 1.8$ mm, indicating that the observed critical diameter satisfies $0.94<d_c<1.8$ mm. For $\delta_0=1.9\times10^{-4}$, $\delta_1=0.87\times10^{-4}$, $g=980$ cm/s^2, $\nu=9.2\times10^{-3}$ cm^2/s, and $D_c=2.0\times10^{-5}$ cm^2/s relevant to these experiments,[9] we predict $d_c=2a_c=1.4$ mm for zero thermal diffusivity (with $\delta=\delta_0$) and $d_c=1.9$ mm for infinite thermal diffusivity (with $\delta=\delta_1$). The predicted results agree with the experimental range, although the latter is slightly higher than the observed upper bound.

The calculations are valid for large and small thermal diffusivity D_T. An important question in making the comparison between theory and experiment is whether the value of D_T for the experiments should be considered

as large or small. Comparison of appropriate length scales provides a possible answer to this question. The cylinder diameter d serves as the vertical length scale of the convective motion for the problem, whereas the thermal thickness $d_T = D_T/c_0$ of the front serves as the length scale over which thermal gradients are significant.[9] In the limit of zero thermal diffusivity $d_T \ll d$, the thermal gradients are confined to the reaction front itself and should have maximum effect on the convective motion. In the limit of infinite thermal diffusivity $d_T \gg d$, the thermal gradients should play no role in the convection. Thus, the crossover from small to large thermal diffusivity would occur at $d_T \approx d$. The experimental values $d = 1$ mm, $D_T = 1.5 \times 10^{-3}$ cm^2/s, and $c_0 = 3 \times 10^{-3}$ cm/s (Ref. 9) imply that $d_T/d \approx 5$, indicating that the thermal diffusivity of the experiments might be considered large. The smooth crossover from small to large D_T described above might also imply a critical diameter that is a monotonic function of D_T. However, verification of these conclusions would require further calculations for finite D_T.

More precise comparisons between theory and experiments would be useful. To make such comparisons, experiments with diameters in the range $0.94 < d < 1.8$ mm and calculations with finite thermal diffusivity are necessary. We intend also to study the mildly nonlinear regime using an amplitude expansion approach to understand the observed front propagation speed enhancements above onset of convection. The transition to chaos provides another potentially fruitful field for research.

ACKNOWLEDGMENTS

Discussions with Kenneth Showalter and support from National Science Foundation Grant No. RII-8922106 and the West Virginia University Energy and Water Research Center are gratefully acknowledged.

[1]T. McManus, Ph.D. thesis, West Virginia University, 1989.

[2]A. Saul and K. Showalter, in *Oscillations and Traveling Waves in Chemical Systems,* edited by R. J. Field and M. Burger (Wiley, New York, 1985), p. 419; N. Ganapathisubramanian and K. Showalter, J. Chem. Phys. **84**, 5427 (1986).

[3]A. Hanna, A. Saul, and K. Showalter, J. Am. Chem. Soc. **104**, 3838 (1982).

[4]G. Bazsa and I. R. Epstein, J. Phys. Chem. **89**, 3050 (1985); I. Nagypál, G. Bazsa, and I. R. Epstein, J. Am. Chem. Soc. **108**, 3635 (1986).

[5]J. J. Tyson and J. P. Keener, Physica D **32**, 327 (1988).

[6]J. A. Pojman and I. R. Epstein, J. Phys. Chem. **94**, 4966 (1990).

[7]J. A. Pojman, I. R. Epstein, T. J. McManus, and K. Showalter, J. Phys. Chem. **95**, 1299 (1991).

[8]J. A. Pojman, I. P. Nagy, and I. R. Epstein, J. Phys. Chem. **95**, 1306 (1991).

[9]B. F. Edwards, J. W. Wilder, and K. Showalter, Phys. Rev. A **43**, 749 (1991).

[10]J. W. Wilder and B. F. Edwards (unpublished).

[11]H. Bénard, Rev. Gen. Sci. Pure Appl. **11**, 1261 (1900); **11**, 1309 (1900); H. Bénard, Ann. Chim. Phys. **23**, 62 (1901); Lord Rayleigh, Philos. Mag. **32**, 529 (1916); **32**, 129 (1965); M. C. Cross, Phys. Fluids **23**, 1727 (1980); B. F. Edwards and A. L. Fetter, *ibid.* **27**, 2795 (1984).

[12]S. Chandrasekhar, *Hydrodynamic and Hydromagnetic Stability* (Oxford University Press, London, 1961), Chap. 2.

[13]S. Chandrasekhar, *Hydrodynamic and Hydromagnetic Stability* (Ref. 12), Appendix V.

[14]W. H. Reid and D. L. Harris, Astrophys. J. Suppl. **3**, 448 (1958).

[15]C. E. Weatherburn, *Differential Geometry of Three Dimensions* (Cambridge University Press, England, 1927), Chap. 4.